Jin Wu
Graduate Research Assistant

Shapour Azarm[1]
Professor

Department of Mechanical Engineering,
University of Maryland,
College Park, MD 20742

Metrics for Quality Assessment of a Multiobjective Design Optimization Solution Set

In this paper, several new set quality metrics are introduced that can be used to evaluate the ''goodness'' of an observed Pareto solution set. These metrics, which are formulated in closed-form and geometrically illustrated, include hyperarea difference, Pareto spread, accuracy of an observed Pareto frontier, number of distinct choices and cluster. The metrics should enable a designer to either monitor the quality of an observed Pareto solution set as obtained by a multiobjective optimization method, or compare the quality of observed Pareto solution sets as reported by different multiobjective optimization methods. A vibrating platform example is used to demonstrate the calculation of these metrics for an observed Pareto solution set. [DOI: 10.1115/1.1329875]

1 Introduction

Real-world engineering design problems often involve concurrent optimization of several incommensurable and competing design objectives [1]. The solution to such problems is usually a set of design alternatives referred to as a Pareto optimal solution set [2]. Many multiobjective optimization methods exist that can be used to generate Pareto solutions. Some of these methods can only generate local Pareto solutions while others such as multiobjective evolutionary methods obtain a ''good'' rather than a true global Pareto solution set [2,3]. As such, it is important for a designer to know how good an observed Pareto solution set is that a multiobjective optimization method obtains. Indeed, knowledge of the goodness of an observed Pareto solution set should enable the designer monitor and potentially improve the performance of a multiobjective optimization method. It should also help the designer compare and contrast the quality of observed Pareto solution sets as reported by different multiobjective optimization methods. The goodness of an observed Pareto solution set, as discussed in this paper, can be evaluated by ''set quality'' metrics.

Relative to other areas in multiobjective optimization, very few papers in the literature have reported on metrics for measuring the set quality of Pareto solutions. Zitzler and Thiele performed a comparative study of four different multiobjective evolutionary methods using two metrics in order to assess the set quality of observed Pareto solution sets. The first metric was the ''size of dominated space'' wherein they defined the size of the objective space that is dominated by a set of Pareto solutions. Given two sets of Pareto solutions, they defined a second metric wherein for each set a fraction of solutions that is dominated by the solutions in the other set is calculated. Van Veldhuizen [5] (wherein further references can be found, e.g., Schott [6] and Srinivas [7]) reviewed and defined nine metrics to assess the quality of Pareto solutions. Under the assumption that the true Pareto solution set is known a priori, Sayin [8] defined the metrics of coverage, uniformity and cardinality in order to assess the quality of a discretely represented Pareto solution set. An assumption made in several of the aforementioned papers is that the true Pareto solution set is known a priori, which is unlikely to be valid for engineering design optimization problems.

In the present paper, the set quality metric named as the ''size of dominated space'' by Zitzler and Thiele [4] is slightly changed and converted to what we call a ''hyperarea difference'' metric. (Van Veldhuizen [5] calls a similar metric as a ''hyperarea'' metric.) For this hyperarea difference metric, a closed-form formula is derived in this paper. In addition, five new set quality metrics are introduced, together with their closed-form formulas. These are: overall Pareto spread, k^{th} objective Pareto spread, accuracy of the observed Pareto frontier, number of distinct choices and cluster. The set quality metrics presented in this paper can be used to assess the goodness of an observed Pareto solution set for a given problem without the knowledge of the true Pareto solution set.

The rest of the paper is organized as follows. Definitions for various terms with their graphical interpretation are given in Section 2. In Section 3, several new set quality metrics are introduced. Design of a vibrating platform is used in Section 4 to demonstrate applicability of the set quality metrics. Finally, the paper is concluded with some remarks in Section 5.

2 Definition and Terminology

The formulation of a typical multiobjective design optimization problem with m objective functions is shown below in Eq. (1).

$$\begin{aligned} &\text{Minimize} \quad f(x)=\{f_1(x),\ldots,f_i(x),\ldots,f_m(x)\} \\ &\text{subject to:} \quad x\in D \\ &D=\{x\in\Re^n: g_j(x)\leqslant 0, j=1,\ldots,J;\ \ h_k(x)=0, k=1,\ldots,K\} \end{aligned} \tag{1}$$

where x is a design vector containing n components of design variables, $f_i(x)$ is the i^{th} objective function, $g_j(x)$ is the j^{th} inequality constraint and $h_k(x)$ is the k^{th} equality constraint. The set of all design vectors which satisfies all constraints is denoted by D. The n-dimensional space wherein its coordinate axes are design variables is referred to as the ''variable space''. The m-dimensional space wherein its coordinate axes are design objective functions is referred to as the ''objective space.''

Ideal Point and Max Point. Typically, the objective space is bounded from below for a minimization problem as in Eq. (1). As such, if each of the objective functions in Eq. (1) is individually minimized subject to the constraints defining the feasible design space D, then an ideal point, $p_I=(f_1^I, f_2^I, \ldots, f_m^I)$, can be obtained in the objective space such that for any feasible point x_k, $x_k\in D$, there exists $f_j^I\leqslant f_j(x_k)$, for all $j=1,\ldots,m$. In contrast, in engineering design problems, there is an upper bound design point in the objective space beyond which even feasible designs are not tolerable. A maximum or a max point defines such a point in the objective space as $p_M=(f_1^M, f_2^M, \ldots, f_m^M)$ such that for any feasible and tolerable design point x_k, $x_k\in D$, there exists $f_j^M \geqslant f_j(x_k)$, for all $j=1,\ldots,m$.

[1]Corresponding author.

Contributed by the Design Automation. Committee for publication in the JOURNAL OF MECHANICAL DESIGN. Manuscript received Jan. 2000. Associate Editor: A. Diaz.

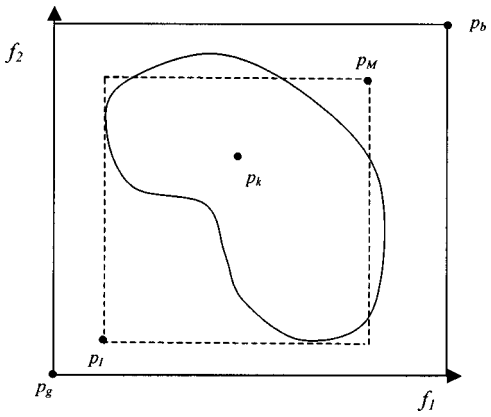

Fig. 1 Good point (p_g), bad point (p_b), ideal point (p_I), and max point (p_M) in the objective space

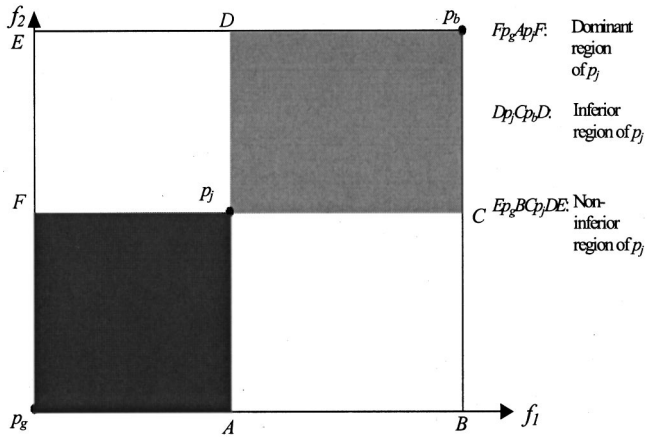

Fig. 2 Dominant, inferior, and non-inferior regions of a point

Good Point and Bad Point. An estimate of the ideal and the max point is referred to as a good and a bad point, respectively. In the context of this paper, it is assumed that in the objective space, a good point estimates the ideal point from below while a bad point estimates the max point from above. In other words, let $p_g=(f_1^g, f_2^g, \ldots, f_m^g)$ and $p_b=(f_1^b, f_2^b, \ldots, f_m^b)$ denote the good point and the bad point in the objective space, respectively. Then, there should always exist $f_j^g \leqslant f_j^I$, and $f_j^b \geqslant f_j^M$ for all $j=1, \ldots, m$. Figure 1 illustrates the definition of the ideal point, the good point, the max point and the bad point in the case of two design objectives.

Scaled Objective Space. All of the objective functions in the objective space are scaled by Eq. (2) so that the scaled good point becomes $p_g=(0, \ldots, 0)$ and the scaled bad point becomes $p_b=(1, \ldots, 1)$.

$$\bar{f}_j(x_k)=\frac{f_j(x_k)-f_j^g}{f_j^b-f_j^g} \tag{2}$$

The hyper-rectangle that is defined by the scaled good and the bad points in the objective space is referred to as a scaled objective space.

Inferior and Dominant Points. Let the two points x_j and x_k in the variable space be denoted by p_j and p_k in the objective space, respectively. If there exists $f_j(x_j) < f_j(x_k)$ for all $j=1, \ldots, m$, one can then state that $p_j \succ p_k$ which means the point p_j is dominant over the point p_k, or the point p_k is inferior to the point p_j.

Pareto Solution Set, True Pareto Solution Set and Observed Pareto Solution Set. The solution (or a discrete representation) to a multi-objective problem is a set of Pareto solutions: $X=(x_1, \ldots, x_{\overline{np}})$ in the variable space wherein for any point $x_j \in X$, there does not exist another point $x_k \in D$ with $k \neq j$, such that $f_i(x_k) \leqslant f_i(x_j)$ for all $i=1, \ldots, m$ with strict inequality for at least one i. In a scaled objective space, the Pareto solution set is written as $P=(p_1, \ldots, p_{\overline{np}})$, where $p_j=(\bar{f}_1(x_j), \ldots, \bar{f}_m(x_j))$, $j=1, \ldots, \overline{np}$, with $\overline{np}$ being the total number of Pareto solutions. In this paper, a Pareto solution set (i.e., generally an infinite set) that truly meets this definition is called a ''true'' Pareto solution set. In contrast, a Pareto solution set that is obtained by a multi-objective optimization method is referred to as an ''observed'' Pareto solution set. In reality, an observed Pareto solution set is an estimate (or a discrete representation) of a true Pareto solution set.

Pareto Frontier. In the objective space, the boundary that is formed by a set of Pareto solutions is referred to as a Pareto frontier. This frontier defines a limit beyond which the Pareto solutions cannot be further improved with respect to all objectives simultaneously.

Extreme Points and Extreme Values. Extreme points are Pareto solutions that have maximum and minimum values for one or more objectives among all Pareto solutions. Extreme values refer to $\bar{f}_{i\,max}$ and $\bar{f}_{i\,min}$ that denote the maximum and minimum scaled values of the i^{th} objective function, respectively, where: $\bar{f}_{i\,\max}=\max_{k=1}^{\overline{np}}(\bar{f}_i(x_k))$ and $\bar{f}_{i\,\min}=\min_{k=1}^{\overline{np}}(\bar{f}_i(x_k))$ for any $x_k \in X$, $X=(x_1, \ldots, x_{\overline{np}})$.

Inferior Region, Non-Inferior Region and Dominant Region of a Point. In a scaled objective space, an inferior region of a point p_j is defined as a hyper-rectangle $S_{in}(p_j)$ such that for all $p_k \in S_{in}(p_j)$, there must be: $p_k \prec p_j$ and $p_k \succ p_b$, or in other words:

$$\bar{f}_i(x_k) > \bar{f}_i(x_j) \quad \text{and} \quad \bar{f}_i(x_k) < 1 \quad \text{for all } i=1, \ldots, m. \tag{3}$$

where $p_k=(\bar{f}_1(x_k), \ldots, \bar{f}_m(x_k))$, $p_j=(\bar{f}_1(x_j), \ldots, \bar{f}_m(x_j))$, $p_b=(1, \ldots, 1)$.

The non-inferior region $S_{nin}(p_j)$ of a point p_j is defined as the complementary region of the p_j's inferior region in the scaled objective space. Let the space (area or volume) of the scaled objective space be unity (with the good point at the zero coordinate point and the bad point at the one), then the non-inferior region of the point p_j is:

$$\text{space}(S_{nin}(p_j))=1-\text{space}(S_{in}(p_j)) \tag{4}$$

Similarly, the dominant region of a point p_j is defined as a hyper-rectangle $S_{do}(p_j)$ such that for all $p_k \in S_{do}(p_j)$, there must be: $p_k \succ p_j$ and $p_k \prec p_g$, or:

$$\bar{f}_i(x_k) < \bar{f}_i(x_j) \quad \text{and} \quad \bar{f}_i(x_k) > 0 \quad \text{for all } i=1, \ldots, m \tag{5}$$

where $p_k=(\bar{f}_1(x_k), \ldots, \bar{f}_m(x_k))$, $p_j=(\bar{f}_1(x_j), \ldots, \bar{f}_m(x_j))$, $p_g=(0, \ldots, 0)$.

As shown in Fig. 2, the region that is defined by its corner points: Fp_gAp_jF, is the dominant region of the point p_j. The region Dp_jCp_bD is the inferior region of the point p_j. Finally, the region Ep_gBCp_jDE is the non-inferior region of p_j.

Inferior Region, Non-inferior Region and Dominant Region of a Pareto Solution Set. For an observed Pareto solution set in the scaled objective space: $P=(p_1, \ldots, p_{\overline{np}})$, the inferior region of the entire observed Pareto solution set $S_{in}(P)$ is defined as the union of the individual Pareto points' inferior region $S_{in}(p_j)$, $j=1, \ldots, \overline{np}$:

$$S_{in}(P)=\bigcup_{j=1}^{\overline{np}} S_{in}(p_j) \tag{6}$$

The non-inferior region $S_{nin}(P)$ of an observed Pareto solution set is defined as the complement of its inferior region in the scaled objective space:

$$\text{space}(S_{nin}(P))=1-\text{space}(S_{in}(P)) \tag{7}$$

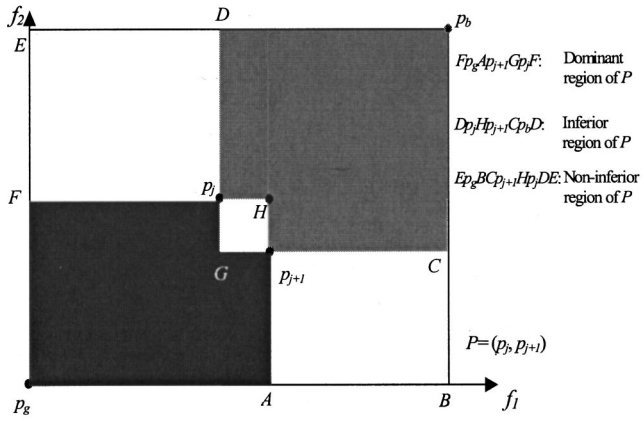

Fig. 3 Dominant, inferior, non-inferior, and observed pareto frontier regions of a set *P*

Using the concept of a point's dominant region, a Pareto set's dominant region $S_{do}(P)$ is defined as the union of Pareto points' dominant regions $S_{do}(p_j)$, $j=1,\ldots,\overline{np}$:

$$S_{do}(P)=\bigcup_{j=1}^{\overline{np}} S_{do}(p_j) \tag{8}$$

As shown in the Fig. 3, the region $Fp_gAp_{j+1}Gp_jF$ is the dominant region of the set P, the region $Dp_jHp_{j+1}Cp_bD$ is the inferior region of the set P, and the region $Ep_gBCp_{j+1}Hp_jDE$ is the non-inferior region of the set P.

3 Quality Metrics

In this section, several set quality metrics are introduced. These quality metrics include hyperarea difference, overall Pareto spread, k^{th} objective Pareto spread, accuracy of the observed Pareto frontier, number of distinct choices and cluster. These metrics could be used, in the objective space, to assess the goodness of an entire observed Pareto solution set.

3.1 Hyperarea Difference (HD). The hyperarea difference metric can be used to quantitatively evaluate the difference between the size of the objective space dominated by an observed Pareto solution set and that of the space dominated by the true Pareto solution set. Note that the true Pareto solution set dominates the entire solution space while an observed Pareto set may only dominate a portion of the solution space. By comparing the size of the dominated (or inferior) solution space of an observed Pareto solution set with that of the true Pareto solution set, a quantitative measure is obtained as to how much worse an observed Pareto solution set is when compared to the true Pareto solution set. Although in reality, the true Pareto solution set is usually unknown, it should still be possible to identify whether or not an observed Pareto solution set is worse than the true Pareto set when compared to another observed Pareto set.

With the concept of inferior region, hyperarea difference can be quantified as the space difference between the inferior region of the true Pareto solution set P_t the inferior region of the observed Pareto solution set P. Let $HD(P)$ represent the hyperarea difference quantity, then:

$$\begin{aligned} HD(P)&=\text{space}(S_{in}(P_t)-S_{in}(P)) \\ &=\text{space}(S_{in}(P_t))-\text{space}(S_{in}(P)) \end{aligned} \tag{9}$$

wherein the term ''space'' refers to the ''area'' in a two-objective space, or ''volume'' in a three or more objective space.

In reality the true Pareto solution set is hardly known a priori to the designer. In that case, the ideal point or the good point can be used as an estimate of the true Pareto solution set. Since if $P_t=\{p_I\}=\{p_g\}$, then: space$(S_{in}(P_t))=1$. Hence, in a scaled objective space, Eq. (9) becomes:

$$HD(P)=1-\text{space}(S_{in}(P))=\text{space}(S_{nin}(P)) \tag{10}$$

In practice, for an m-dimensional objective space, computing the space of a set's non-inferior region directly can be cumbersome. According to Eqs. (6) and (10), computing the space of an observed Pareto set's inferior region can be converted to a problem of computing the union of the space formed by the inferior regions for an $\overline{np}$ number of points. For instance, in a simple case wherein there are three points in the observed Pareto solution set, i.e., $P=(p_1,p_2,p_3)$. The union of the space of the inferior regions for these three points is:

$$\begin{aligned} &\text{space}(S_{in}(P)) \\ &\quad=\text{space}(S_{in}(p_1)\cup S_{in}(p_2)\cup S_{in}(p_3)) \\ &\quad=\text{space}(S_{in}(p_1))+\text{space}(S_{in}(p_2))+\text{space}(S_{in}(p_3)) \\ &\qquad-\text{space}(S_{in}(p_1)\cap S_{in}(p_2))-\text{space}(S_{in}(p_1)\cap S_{in}(p_3)) \\ &\qquad-\text{space}(S_{in}(p_2)\cap S_{in}(p_3)) \\ &\qquad+\text{space}(S_{in}(p_1)\cap S_{in}(p_2)\cap S_{in}(p_3)) \end{aligned} \tag{11}$$

In general, Eq. (12) can be used to calculate space$(S_{in}(p_k))$ for an m-dimensional scaled objective space:

$$\text{space}(S_{in}(p_k))=\prod_{i=1}^{m}\left[1-\overline{f}_i(x_k)\right] \tag{12}$$

Calculating the intersection of the r number of solution points' inferior regions ($r\leq\overline{np}$) can be accomplished by:

$$\text{space}\left(\bigcap_{j=1}^{r} S_{in}(p_j)\right)=\prod_{i=1}^{m}\left[1-\max_{j=1}^{r}(\overline{f}_i(x_j))\right] \tag{13}$$

Therefore

$$\begin{aligned} &\text{space}(S_{in}(P)) \\ &\quad=\sum_{r=1}^{\overline{np}}\text{space}(S_{in}(P_r))-\sum_{r<t}\text{space}(S_{in}(P_r)\cap S_{in}(P_t)) \\ &\qquad+\sum_{r<t<u}\text{space}(S_{in}(P_r)\cap S_{in}(P_t)\cap S_{in}(P_u)) \\ &\qquad-\sum_{r<t<u<s}\text{space}(S_{in}(P_r)\cap S_{in}(P_t)\cap S_{in}(P_u\cap S_{in}(P_s)) \\ &\qquad+\ldots+(-1)^{\overline{np}+1}\text{space}(S_{in}(P_1)\cap S_{in}(P_2) \\ &\qquad\times\cap\ldots\cap S_{in}(P_{\overline{np}})) \end{aligned} \tag{14}$$

Mathematically, the hyperarea difference becomes:

$$\begin{aligned} HD(P)&=1-\text{space}(S_{in}(P)) \\ &=1-\left\{\sum_{r=1}^{\overline{np}}\left\{(-1)^{r+1}\right.\right. \\ &\qquad\times\left[\sum_{k_1=1}^{\overline{np}-r+1}\cdots\sum_{k_l=k_{l-1}+1}^{\overline{np}-(r-l+1)+1}\cdots\right. \\ &\qquad\left.\left.\left.\times\sum_{k_r=k_r-1}^{\overline{np}}\prod_{i=1}^{m}\left[1-\max_{j=1}^{r}(\overline{f}_i(x_{k_j}))\right]\right]\right\}\right\} \end{aligned} \tag{15}$$

For instance, to calculate the hyperarea difference of an observed Pareto solution set $P=(p_1,p_2,p_3)$, Eq. (15) becomes:

$$
\begin{aligned}
HD(P) &= 1-\text{space}(S_{in}(P)) \\
&= 1-\Bigg\{ (-1)^{1+1}\sum_{k_1=1}^{3}\prod_{i=1}^{m}\left[1-\max_{j=1}^{1}(\overline{f}_i(x_{k_j}))\right] \\
&\quad +(-1)^{2+1}\sum_{k_1=1}^{3-2+1}\sum_{k_2=k_1+1}^{3-(2-2+1)+1}\prod_{i=1}^{m}\left[1-\max_{j=1}^{2}(\overline{f}_i(x_{k_j}))\right] \\
&\quad +(-1)^{3+1}\sum_{k_1=1}^{3-3+1}\sum_{k_2=k_1+1}^{3-(3-2+1)+1}\sum_{k_3=k_2+1}^{3}\prod_{i=1}^{m} \\
&\quad \times\left[1-\max_{j=1}^{3}(\overline{f}_i(x_{k_j}))\right]\Bigg\} \\
&= 1-\Bigg\{ \sum_{k_1=1}^{3}\prod_{i=1}^{m}\left[1-\max_{j=1}^{1}(\overline{f}_i(x_{k_j}))\right] \\
&\quad -\sum_{k_1=1}^{2}\sum_{k_2=k_1+1}^{3}\prod_{i=1}^{m}\left[1-\max_{j=1}^{2}(\overline{f}_i(x_{k_j}))\right] \\
&\quad +\sum_{k_1=1}^{1}\sum_{k_2=k_1+1}^{2}\sum_{k_3=k_2+1}^{3}\prod_{i=1}^{m}\left[1-\max_{j=1}^{3}(\overline{f}_i(x_{k_j}))\right]\Bigg\} \qquad (16)
\end{aligned}
$$

Using the hyperarea difference quality metric, Eq. (15), different observed Pareto solution sets can be compared with one another quantitatively. In general, an observed Pareto solution set with a lower hyperarea difference value is considered to be better than the one with a higher hyperarea difference value.

3.2 Pareto Spread. The quality metrics under Pareto spread are to address the range of objective function values. An observed Pareto solution set that spreads over a wider range of the objective function values provides the designer with broader optimized design choices. Pareto spread is quantified by two metrics: (i) the overall Pareto spread, and (ii) the k^{th} objective Pareto spread.

3.2.1 Overall Pareto Spread (OS). The overall Pareto spread metric quantifies how widely the observed Pareto solution set spreads over the objective space when the design objective functions are considered altogether. This metric is defined as the volume ratio of two hyper-rectangles. One of these rectangles is HR_{gb} that is defined by the good and bad points with respect to each design objective. Similarly, the extreme points for an observed Pareto solution set defines the other hyper-rectangle that is denoted by HR_{ex}. The overall Pareto spread is defined as the ratio of the area or volume of HR_{ex} to that of HR_{gb}:

$$
OS(P)=\frac{HR_{ex}(P)}{HR_{gb}} \qquad (17)
$$

where P refers to an observed Pareto solution set. By using the objective values to interpret $HR_{ex}(P)$ and HR_{gb}, Eq. (17) can be expressed as:

$$
\begin{aligned}
OS(P) &= \frac{\prod_{i=1}^{m}\left|\max_{k=1}^{np}(p_k)_i-\min_{k=1}^{np}(p_k)_i\right|}{\prod_{i=1}^{m}\left|(p_b)_i-(p_g)_i\right|} \\
&= \prod_{i=1}^{m}\left|\max_{k=1}^{np}[\overline{f}_i(x_k)]-\min_{k=1}^{np}[\overline{f}_i(x_k)]\right| \qquad (18)
\end{aligned}
$$

For example, in a two-objective space shown in Fig. 4, the overall Pareto spread is calculated as:

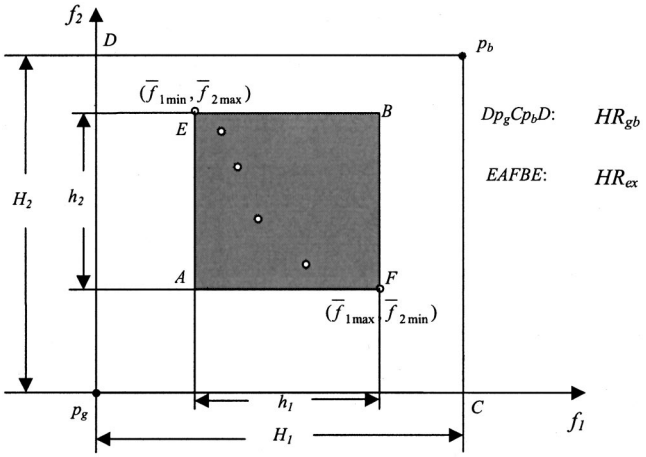

Fig. 4 Overall pareto spread and k^{th} pareto spread

$$
OC(P)=\frac{h_1h_2}{H_1H_2} \qquad (19)
$$

where $h_1=|\overline{f}_{1\max}-\overline{f}_{1\min}|$, $h_2=|\overline{f}_{2\max}-\overline{f}_{2\min}|$, $H_1=|(p_g)_1-(p_b)_1|$ and $H_2=|(p_g)_2-(p_b)_2|$. When comparing two observed Pareto solution sets P_1 and P_2, the designer prefers the one with a wider spread. In other words, if $OS(P_1)>OS(P_2)$, then the solution set P_1 is preferred to P_2.

3.2.2 k^{th} Objective Pareto Spread (OS_k). The overall Pareto spread metric is simple in the sense that by using Eq. (17), the designer can have some knowledge about the overall range of the solution set. However, the overall Pareto spread does not provide any insight into the range of the solution set with respect to each individual design objective. The k^{th} objective Pareto spread OS_k is introduced as an additional metric to the overall Pareto spread metric aiming at quantitatively depicting the solution range with respect to each individual design objective. The k^{th} objective Pareto spread metric, $k=1,\ldots,m$, is defined as:

$$
\begin{aligned}
OS_k(P) &= \frac{\left|\max_{i=1}^{np}((p_i)_k)-\min_{i=1}^{np}((p_i)_k)\right|}{\left|(p_b)_k-(p_g)_k\right|} \\
&= \left|\max_{i=1}^{np}(\overline{f}_k(x_i))-\min_{i=1}^{np}(\overline{f}_k(x_i))\right| \qquad (20)
\end{aligned}
$$

By using Eq. (20), the observed Pareto solutions shown in Fig. 4 has the 1st and 2nd objective Pareto spread value, as follows:

$$
OS_1(P)=\frac{h_1}{H_1}=|\overline{f}_{1\max}-\overline{f}_{1\min}| \qquad (21)
$$

and

$$
OS_2(P)=\frac{h_2}{H_2}=|\overline{f}_{2\max}-\overline{f}_{2\min}| \qquad (22)
$$

Using the k^{th} objective Pareto spread (OS_k) to compare two observed Pareto solution set, if $OS_k(P_1)>OS_k(P_2)$, one can conclude that the solution set P_1 is preferred to P_2 with respect to the k^{th} objective spread.

3.3 Accuracy of the Observed Pareto Frontier (AC). Once an observed Pareto solution set (i.e., a discrete set in its nature) is obtained, its corresponding observed Pareto frontier can be estimated. Knowledge of an observed Pareto frontier in addition to the observed Pareto solution set may become important to a designer dealing with real-world engineering problems. The more accurate the observed Pareto frontier is estimated, the more knowledge the designer gains about the nature of the Pareto design solutions and tradeoffs that exist between such solutions.

According to the definitions for the inferior and dominant regions of an observed Pareto solution set $P=(p_1,\ldots,p_{\overline{np}})$, if there exist additional observed Pareto solutions that are undetected, then such solutions have to be non-inferior with respect to the current observed Pareto solutions and thus could not belong to either the observed Pareto solution set's inferior region ($S_{in}(P)$) or dominant region ($S_{do}(P)$). Indeed, such undetected observed Pareto solutions have to belong to a region that is left over from the scaled objective spacer after the inferior and dominant regions are subtracted from it. Let the quantity $AP(P)$ denotes the region wherein an observed Pareto frontier falls into for an observed Pareto solution set P. The quantity $AP(P)$ is defined as the frontier approximation of the observed Pareto solution set P. The impreciseness of the approximation comes from the fact that not all the points in the region can be simultaneously on the Pareto frontier. When the approximation gets more and more accurate to the level where it eventually becomes the true Pareto frontier, the impreciseness will vanish. The quantity $AP(P)$ is obtained as follows:

$$AP(P)=1-\text{space}(S_{in}(P))-\text{space}(S_{do}(P)) \tag{23}$$

Figure 4 gives a graphical interpretation of the metric $AP(P)$ which essentially is the space (area or volume) difference of non-inferior and dominant regions for an observed Pareto solution P. Calculating the value of the quantity $AP(P)$, as shown in Eq. (23), involving computing the volume of the Pareto solution set P's inferior and dominant regions. From the derivation for the hyperarea difference in Section 3.1, the set P's inferior region is:

$$\begin{aligned}&\text{space}(S_{in}(P))\\&=\sum_{r=1}^{\overline{np}}\left\{(-1)^{r+1}\left[\sum_{k_1=1}^{\overline{np}-r+1}\cdots\sum_{k_l=k_{l-1}+1}^{\overline{np}-(r-l+1)+1}\cdots\right.\right.\\&\left.\left.\times\sum_{k_r=k_r-1}^{\overline{np}}\prod_{i=1}^{m}\left[1-\max_{j=1}^{r}(\overline{f_i}(x_{k_j}))\right]\right]\right\}\end{aligned} \tag{24}$$

and the set P's dominant region is:

$$\begin{aligned}&\text{space}(S_{do}(P))\\&=\sum_{r=1}^{\overline{np}}\left\{(-1)^{r+1}\left[\sum_{k_1=1}^{\overline{np}-r+1}\cdots\sum_{k_l=k_{l-1}+1}^{\overline{np}-(r-l+1)+1}\cdots\right.\right.\\&\left.\left.\times\sum_{k_r=k_r-1}^{\overline{np}}\prod_{i=1}^{m}\left[1-\min_{j=1}^{r}(\overline{f_i}(x_{k_j}))\right]\right]\right\}\end{aligned} \tag{25}$$

Let $AC(P)$ denote the value of the quality metric ''accuracy of the observed Pareto frontier''. Then the quantity $AC(P)$ is defined as:

$$AC(P)=\frac{1}{AP(P)} \tag{26}$$

When an observed Pareto solution set is empty, the designer has the least (zero) amount of knowledge about the corresponding Pareto frontier. In this case and according to Eq. (21): $AP(P)=1$, and $AC(P)=1$. In the other extreme case when the observed Pareto solution set contains all of the Pareto solutions belonging to the observed Pareto frontier, and the Pareto frontier is continuous, then $AP(P)=0$, and $AC(P)=\infty$. When comparing two observed Pareto solution sets, the set with a higher value of the quantity $AC(P)$ is preferred to the one with a lower value.

3.4 Number of Distinct Choices (NDC_μ). From a designer's point of view, the more is the number of points contained in an observed Pareto solution set, the more is the number of design options to choose from. However, if the observed Pareto solutions are too close to one another in the objective space, then the variations between the observed Pareto solutions may be indistinguishable to the designer. In other words, the more number of observed Pareto solutions does not necessarily mean that the more is the number of design choices. In short, for an observed Pareto solution set $P=(p_1,\ldots,p_{\overline{np}})$, only those solutions that are sufficiently distinct from one another should be accounted for as useful design options.

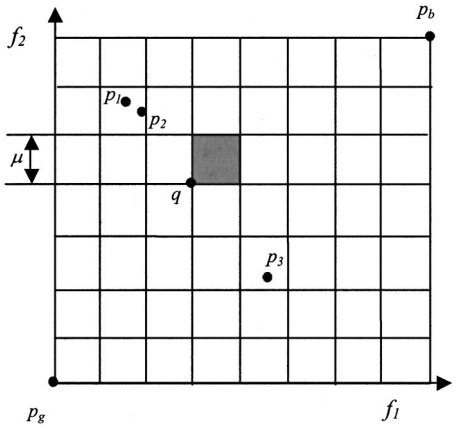

Fig. 5 Indifference region $T_\mu(q)$, as shown by a shaded grid

Let the quantity μ $(0<\mu<1)$ be a number specified by the designer, which can be used to divide an m-dimensional objective space into $1/\mu^m$ number of small grids. For simplicity, $1/\mu$ is taken to be as an integer. Each of the grids refers to a square (hyper-cube in m-dimension), the indifference region $T_{\mu(q)}$, wherein any two solution points p_i and p_j within the region are considered similar to one another or that the designer is indifferent to such solutions. Figure 5 illustrates the quantity μ and $T_\mu(q)$ in a two-dimensional objective space.

Let the quantity $NT_\mu(q,P)$ indicate whether or not there is any point $p_k\in P$ that falls into the region $T_\mu(q)$. The quantity $NT_\mu(q,P)$ will be equal to unity (or 1) as long as there is at least one solution point p_k falling into the indifference region $T_\mu(q)$. The quantity $NT_\mu(q,P)$ will be equal to zero (or 0) as long as there is no solution falling into the region $T_\mu(q)$. In general, $NT_\mu(q,P)$ can be stated as:

$$NT_\mu(q,P)=\begin{cases}1 & \exists p_k\in P \quad p_k\in T_\mu(q)\\ 0 & \forall p_k\in P \quad p_k\notin T_\mu(q)\end{cases} \tag{27}$$

The quality metric $NDC_\mu(P)$, that is the number of distinct choices for a pre-specified value of μ, can then be defined as:

$$\begin{aligned}&NDC_\mu(P)=\sum_{l_m=0}^{\nu-1}\cdots\sum_{l_2=0}^{\nu-1}\sum_{l_1=0}^{\nu-1}NT_\mu(q,P)\\&\text{where}\quad q=(q_1,q_2,\ldots,q_m)\ \text{with}\ q_i=\frac{l_i}{\nu}\end{aligned} \tag{28}$$

wherein $\nu=1/\mu$. The point q, located at any intersection of m-grid lines in the objective space, has coordinates $(q_1,q_2,\ldots,q_m)$. As illustrated at the beginning of this section, for a pre-specified value of μ, an observed Pareto solution set with a higher value of the quantity $NDC_\mu(P)$ is preferred to a set with a lower value.

3.5 Cluster (CL_μ). The quality metric of the previous section, i.e., the number of distinct choices (NDC_μ), indicates the number of distinct solutions that exists in an observed Pareto solution set. By using this quality metric alone, however, the cluster phenomenon can not be properly interpreted. For instance, suppose for a pre-specified value of μ, the observed Pareto solution set P_1 provides 10 distinct solutions with $NDC_\mu=10$. Suppose now that there is also another observed Pareto solution set P_2 with 100 solutions with $NDC_\mu=10$. It can be observed that the solu-

tion set P_2 is not desirable by the designer since many of the solutions in this set are likely to be clustered. Hence, the quality metric cluster, $CL_\mu(P)$, is introduced:

$$CL_\mu(P)=\frac{N(P)}{NDC_\mu(P)} \tag{29}$$

where $N(P)$ is the number of the observed Pareto solutions. In the ideal case where every Pareto solution obtained is distinct, then the value of the quantity $CL_\mu(P)$ is equal to 1. In all other cases, $CL_\mu(P)$ is greater than 1. Also, the higher the value of the cluster quantity $CL_\mu(P)$ is, the more clustered the solution set is, and hence the less preferred the solution set.

4 Example

The purpose of this section is to numerically illustrate the proposed set quality metrics using a simple two-objective engineering design optimization example: design of a vibrating platform.

4.1 Vibrating Platform: Problem Description With an Observed Pareto Solution Set. This example was adopted from Messac [9] with some modifications. It consists of a pinned-pinned sandwich beam with a vibrating motor on its top. As shown in Fig. 6, the beam has five layers of three different materials. There is a middle layer and two sandwich layers. The distance from the center of the beam to the outer edge of each layer comprises three of the sizing design variables, d_1, d_2, d_3. The width of the beam b and the length of the beam L are the other two sizing design variables. There are also three combinatorial variables for the material type M_i, where $i=1,2,3$, for the different materials that can be used for each layer. Hence, there are 8 design variables, which consist of 3 combinatorial variables for the material type of the 3 layers and 5 sizing variables.

The two design objectives are to maximize the fundamental frequency of the beam, and to minimize the material cost. The maximization of the fundamental frequency is converted to a minimization form by minimizing the negative of the fundamental frequency. The problem formulation is shown below:

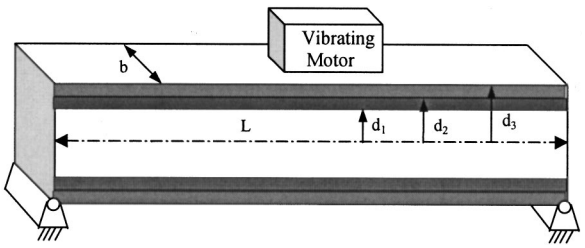

Fig. 6 Vibrating platform example

$$\begin{aligned}
&\text{Minimize } f_1(d_1,d_2,d_3,b,L,M_i)=-(\pi/2L^2)(EI/\mu)^{0.5}\\
&(EI)=(2b/3)[E_1d_1^3+E_2(d_2^3-d_1^3)+E_3(d_3^3-d_2^3)]\\
&(\mu)=2b[\rho_1d_1+\rho_2(d_2-d_1)+\rho_3(d_3-d_2)]\\
&\text{Minimize } f_2(d_1,d_2,d_3,b,L,M_i)\\
&\quad=2b[c_1d_1+c_2(d_2-d_1)+c_3(d_3-d_2)]\\
&\text{Subject to: } g_1:\ \mu L-2800\leqslant 0\\
&\qquad g_2:\ d_2-d_1-0.15\leqslant 0\\
&\qquad g_3:\ d_3-d_2-0.01\leqslant 0\\
&\qquad 0.05\leqslant d_1\leqslant 0.5\\
&\qquad 0.2\leqslant d_2\leqslant 0.5\\
&\qquad 0.2\leqslant d_3\leqslant 0.6\\
&\qquad 0.35\leqslant b\leqslant 0.5\\
&\qquad 3\leqslant L\leqslant 6
\end{aligned} \tag{30}$$

Here, E_i is the modulus of elasticity of material M_i, while ρ_i is the density, and c_i is the cost. According to the material type variable M_i, the value of the parameters E_i, ρ_i, and c_i are different for different layer material, as given in Table 1. It is assumed that the material types for the three layers are mutually exclusive. In other words, the same material cannot be used for more than one layer. However, the layers are allowed to have zero thickness. The first three constraints refer to upper bounds on the mass of the beam, thickness of layer 2, and thickness of layer 3, respectively, and they are labeled g_1 through g_3. The last 5 constraints are the set constraints on the sizing variables [10].

By using a multiobjective optimization method [10], three Pareto solutions are observed. The observed Pareto solution values and the good and bad values are given in Table 2. These values are scaled so that the good and bad points are at (0,0) and (1,1), respectively.

4.2 Quality of the Observed Pareto Solution Set. In order to assess the quality of the observed Pareto solution set P, the value of the quality metrics introduced in Section 3 are computed in the scaled objective space.

The hyperarea difference metric refers to the area of the non-inferior region of the observed Pareto set. By using Eq. (15), hyperarea difference can be calculated as follows:

$$\begin{aligned}
HD(P)=1-[&((1-0.26)\times(1-0.68)+(1-0.28)\times(1-0.65)\\
&+(1-0.7)\times(1-0.24))+((1-0.28)\times(1-0.68)\\
&+(1-0.7)\times(1-0.65)+(1-0.7)\times(1-0.68))\\
&+((1-0.07)\times(1-0.68))]\\
=0.6186&
\end{aligned} \tag{31}$$

Table 1 Layer material properties of the vibrating platform example

Material M_i	ρ_i (Kg/m^3)	E_i (N/m^2)	C_i (\$/volume)
1	100	1.6×10^9	500
2	2,770	70×10^9	1,500
3	7,780	200×10^9	800

Table 2 Good and bad points and the three Pareto solutions in the vibrating platform example

Pareto solution	Frequency	Cost	Scaled Frequency	Scaled Cost
p_1	-363.7	167.9	0.26	0.68
p_2	-357.9	165.1	0.28	0.65
p_3	-265.1	123.8	0.70	0.24
Good point p_g	-420	100	0	0
Bad point p_b	-200	200	1	1

Table 3 (*a*) The observed Pareto solution set P_1 by using I-SHOT [10]; (*b*) the observed pareto solution set P_2 by using MOGA [10]

Pareto solution	Frequency	Cost	Scaled Frequency	Scaled Cost
p_1	-400.734	184.260	0.088	0.843
p_2	-396.671	182.937	0.106	0.829
p_3	-363.778	167.959	0.256	0.680
p_4	-351.899	165.111	0.310	0.651
p_5	-317.219	148.132	0.467	0.481
p_6	-265.168	123.824	0.704	0.238
p_7	-219.723	102.244	0.910	0.022
Good point p_g	-420	100	0	0
Bad point p_b	-200	200	1	1

Pareto solution	Frequency	Cost	Scaled Frequency	Scaled Cost
p_1	-388.125	199.692	0.145	0.997
p_2	-363.332	192.793	0.258	0.928
p_3	-326.017	159.496	0.427	0.595
p_4	-320.859	157.597	0.451	0.576
p_5	-299.300	151.005	0.549	0.510
p_6	-289.273	150.546	0.594	0.505
p_7	-259.578	133.528	0.729	0.335
p_8	-219.629	132.323	0.911	0.323
p_9	-215.992	120.642	0.927	0.206
Good point p_g	-420	100	0	0
Bad point p_b	-200	200	1	1

By applying Eq. (18), the metric for overall Pareto spread is computed:

$$OS(P)=\frac{HR_{ex}(P)}{HR_{gb}}=(0.7-0.26)\times(0.68-0.24)=0.194 \tag{32}$$

Since there are two design objectives, the metrics for the 1st objective Pareto spread and the 2nd objective Pareto spread can be calculated by using Eq. (20). They are:

$$OS_1(P)=0.7-0.26=0.44 \tag{33}$$

$$OS_2(P)=0.68-0.24=0.44 \tag{34}$$

To calculate the accuracy of the approximated Pareto frontier, both the area of the Pareto set's inferior region and dominant region should be calculated first. The area of the Pareto solution set P's inferior region is $space(S_{in}(P))=1-CD(P)=1-0.6186=0.3814$. Its dominant region can be calculated by using Eq. (25) as shown below:

$$\begin{aligned}\text{space}(S_{do}(P))&=(0.26\times0.68+0.28\times0.65+0.7\times0.24)\\&\quad-(0.26\times0.65+0.26\times0.24+0.28\times0.24)\\&\quad+(0.26\times0.24)\\&=0.2906\end{aligned} \tag{35}$$

According to Eq. (23) and Eq. (26), the accuracy of the observed Pareto frontier is:

$$AC(P)=\frac{1}{AP(P)}=\frac{1}{1-\text{space}(S_{in})-\text{space}(S_{do})}=\frac{1}{1-0.3814-0.2906}=3.05 \tag{36}$$

For a pre-specified value of $\mu=0.1$, the two-objective space is divided into 100 indifference regions wherein within each indifference region, the observed Pareto solutions are regarded to be the same. By applying Eqs. (27) and (28), the number of distinct design choices is obtained:

$$NDC_{0.1}=2 \tag{37}$$

By using Eq. (29), the value of the cluster metric is:

$$CL_{0.1}(P)=\frac{N(P)}{NDC_{0.1}(P)}=\frac{3}{2} \tag{38}$$

Two sets of Pareto solutions, as shown in Table 3, are observed by using two multiobjective optimization procedures reported in Azarm et al. [10]. The graphical results are shown in Fig. 7. By applying the suggested quality metrics, the quantitative information about the goodness of these observed Pareto solutions can be easily calculated. The quality results are shown in Table 4. From Fig. 7, one can see that the observed Pareto solution set P_1 is closer to the ideal points and generally preferred by the designers. This conclusion agrees with the values of the quality metrics.

As one can see from this example, the set quality metrics can be easily computed and applied for assessing the quality of any observed Pareto solution set. By using these quality metrics, the

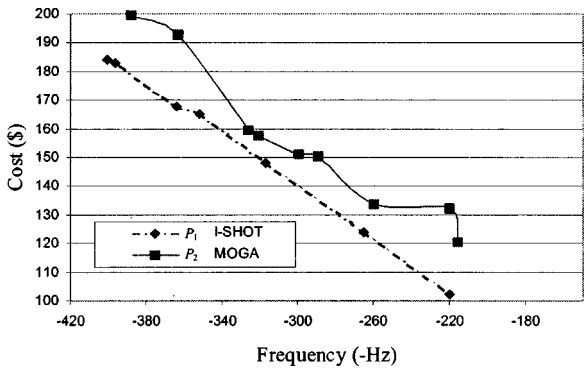

Fig. 7 Two sets of observed Pareto solutions

Table 4 The quality of the observed Pareto sets P_1 and P_2

Observed Pareto Solution Set	HD	OS	OS_k		AC	NDC_μ (μ=0.1)	CL_μ (μ=0.1)
			OS_1	OS_2			
P_1	0.53	0.68	0.82	0.82	5.92	7	1
P_2	0.66	0.62	0.78	0.79	8.77	7	1.29

degree by which an observed Pareto solution set satisfies the designer's preferences can be quantitatively interpreted.

5 Conclusion

The set quality metrics presented in this paper provide a means to measure the goodness of an observed Pareto solution set. These metrics include 1) hyperarea difference, 2) overall Pareto spread, 3) k^{th} objective Pareto spread, 4) accuracy of the observed Pareto frontier, 5) number of distinct choices, and 6) cluster.

The hyperarea difference metric quantifies the non-inferior region or how much of the scaled objective space is dominated by an observed Pareto solution set or how much worse an observed Pareto solution set is when compared to the true Pareto solution set. The overall Pareto spread metric indicates how wide an observed Pareto solution set spreads over the objective space with respect to all objectives as a whole. The k^{th} objective Pareto spread metric indicates how wide an observed Pareto solution set spreads over the objective space with respect to individual objectives. The metric for the accuracy of the observed Pareto frontier indicates how good an observed Pareto solution set estimates a corresponding Pareto frontier. The metric for the number of distinct choices indicates the number of distinguishable design options in an observed Pareto solution set. The cluster metric indicates how dense the solutions are in an observed Pareto solution set. In general, the lower the values of the metrics for hyperarea difference and cluster and the higher the values of the metrics for Pareto spread, accuracy of the observed Pareto frontier and number of distinct choices are, the more preferred is an observed Pareto solution set.

The set quality metrics of this paper can also be used to compare the goodness of observed Pareto solutions as reported by different multiobjective optimization methods. This means that by using these metrics, the quality of various multiobjective optimization methods can be compared against one another. The metrics may also be used as a dynamic monitoring tool (e.g., as stopping criteria) for a multiobjective optimization method.

Acknowledgments

The work presented in this paper was supported in part by NSF (DMI-9700059) and ONR (N0001498108492), and in part by Maryland Industrial Partnerships and IHDIV-NSWC. Such support does not constitute an endorsement by the funding agency of the opinions expressed in the paper. The input of A. Kurapati with regard to the quality metrics for hyperarea difference and overall Pareto spread is also acknowledged.

References

[1] Eschenauer, C. M., Koski, J., and Osyczka, A., eds., 1990, *Multicriteria Design Optimization*, Springer-Verlag, New York.

[2] Miettinen, K. M., 1999, *Nonlinear Multiobjective Optimization*, Kluwer Academic, Boston.

[3] Bäck, T., 1996, *Evolutionary Algorithms in Theory and Practice*, Oxford University Press, New York.

[4] Zitzler, E., and Thiele, L., 1998, ''Multiobjective Optimization Using Evolutionary Algorithms—A Comparative Case Study,'' In Eiben, A. E., et al., *Proc. 5th International Conference: Parallel Problem Solving from Nature—PPSNV*, Amsterdam, The Netherlands, Springer, pp. 292–301.

[5] Van Veldhuizen, D. A., 1999, ''Multiobjective Evolutionary Algorithm: Classifications, Analyses, and New Innovations,'' Ph.D. Dissertation, Department of Electrical and Computer Engineering, Air Force Institute of Technology, Wright-Patterson AFB, Ohio.

[6] Schott, J. R., 1995, ''Fault Tolerant Design Using Single and Multicriteria Genetic Algorithm Optimization,'' MS Thesis, Department of Aeronautics and Astronautics, MIT, Cambridge, Massachusetts.

[7] Srinivas, N., and Deb, K., 1994, ''Multiobjective Optimization Using Nondominated Sorting in Genetic Algorithm,'' Evolu. Comput., **2**, No. 3, pp. 221–248.

[8] Sayin, S., 1997, ''Measuring the Quality of Discrete Representations of Efficient Sets in Multiple Objective Mathematical Programming,'' Working Paper No. 1997/25, Koç University, Turkey.

[9] Messac, A., 1996, ''Physical Programming: Effective Optimization for Computational Design,'' AIAA J., **34**, No. 1, pp. 149–158.

[10] Azarm, S., Reynolds, B., and Narayanan, S., 1999, ''Comparison of Two Multiobjective Optimization Techniques with and within Genetic Algorithm,'' *CD-ROM Proceedings of the ASME DETC, Design Automation Conference*, Paper No. DETC99/DAC-8584, DETC'99 September 12–16, 1999, Las Vegas, Nevada.